

# Reconstruction of cellular forces in fibrous biopolymer network

Yunsong Zhang,<sup>1</sup> Jingchen Feng,<sup>2</sup> Shay Heizler,<sup>3</sup> and Herbert Levine<sup>2</sup>

<sup>1</sup>*Department of Physics & Astronomy and Center for Theoretical Biological Physics, Rice University, Houston TX, 77251-1892, USA.*

<sup>2</sup>*Center for Theoretical Biological Physics, Rice University, Houston TX, 77251-1892, USA*

<sup>3</sup>*Nuclear Research Center, Negev, Department of Physics P.O.Box 9001, Beer Sheva 84190, Israel*

(Dated: December 9, 2024)

How cells move through 3d extracellular matrix (ECM) is of increasing interest in attempts to understand important biological processes such as cancer metastasis. Just as in motion on 2d surfaces, it is expected that experimental measurements of cell-generated forces will provide valuable information for uncovering the mechanisms of cell migration. Here, we use a lattice-based mechanical model of ECM to study the cellular force reconstruction issue. We conceptually propose an efficient computational scheme to reconstruct cellular forces from the deformation and explore the performance of our scheme in presence of noise, varying marker bead distribution, varying bond stiffnesses and changing cell morphology. Our results show that micromechanical information, rather than merely the bulk rheology of the biopolymer networks, is essential for a precise recovery of cellular forces.

## I. INTRODUCTION

The migration of eukaryotic cells in complex environments plays a significant role in many biological processes, such as embryonic morphogenesis, immune defense, and tumor invasion [1]. One widely encountered biomechanical environment for migrating eukaryotic cells *in vivo* is the three-dimensional (3D) extracellular matrix (ECM), composed of a dense network of biopolymers such as collagen and fibrin [2]. To make their ways through ECM, cells apply a variety of different strategies, involving mechanisms of cytoskeleton force generation, protease production, and cell adhesions. Whatever strategy cells use, cell-generated forces acting on the ECM are valuable clues to infer what is happening within a migrating 3D cell.

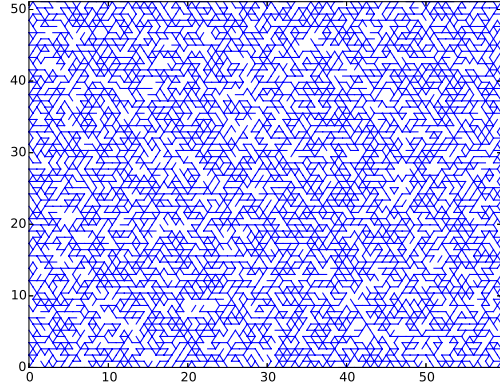
Recently, experimental advances have been made in quantifying the ECM's response to migrating cells [3–6]. In these experimental setups, cells are often cultured in artificially synthesized extracellular matrix (ECM), such as type I collagen gel, which efficiently mimics the environment in living tissues [7]. As the cells migrate, they deform the surrounding environment; this deformation is trackable by for example placing marker beads in the gel. However, from a theoretical perspective, a gap still exists between knowing the deformation of the ECM and determining what forces cells have exerted on that ECM. The inversion from the former to the latter remains elusive, because the ECM display very complex properties such as strain-stiffening [8], non-affine deformations.

In a recent work, Steinwachs *et al* attempted a reconstruction scheme based on a continuous elasticity model, which phenomenologically captures the strain-stiffening property of collagen gels [6]. This effort goes beyond previous approaches which used linear elastic assumptions and hence represents a step forward [3, 4, 9]. However it remains unclear how accurately this method would capture the mechanics of a real biopolymer network. In particular real networks are expected to exhibit microme-

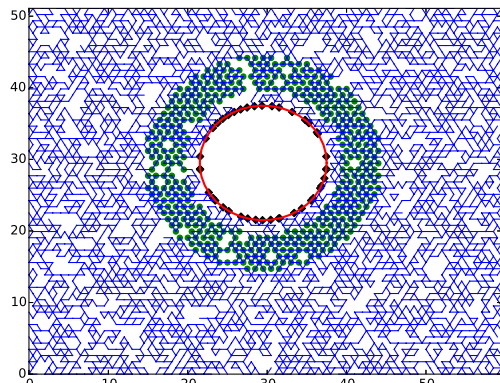
chanical fluctuations [10] in its properties on the scale of the network elements which are not very different than the scale of the embedded cell. Therefore, a more detailed understanding of ECM networks is essential for a quantitatively successful reconstruction of cellular forces in 3D ECM.

Here, we use a lattice-based mechanical model to study this force reconstruction problem. In particular, we make use of recent progress in the soft-matter physics community towards the understanding of the ECM systems [11]. It has been shown that these systems can be modeled as a disordered network of semiflexible polymers with an interplay between bond stretching and bending. On the basis of this idea, computational models have been built to capture the critical properties such as strain stiffening, negative normal stress, and non-affine deformations. These models roughly fall into two categories: lattice-based models [12–20] and off-lattice models (Mikado network)[20–28]. The former places straight fibers on a regular lattice; these fibers are determined by straight segments of bonds on a diluted network. The other approach consists of placing stochastically positioned fibers, intersecting with each other and forming crosslinks; this is usually referred to as a Mikado model. As in both of these cases the mechanics is controlled by critical behavior [12, 18, 20] around the Maxwell point (at which bending becomes the dominant response mechanism at small strain), the results from these different approaches are extremely consistent with each other [29, 30]. In this paper, we study a reconstruction scheme based on a two-dimensional (2D) diluted lattice model. We chose the lattice model for its computational efficiency, In addition, the fact, that lattice-based model in both 2D and 3D exhibit nearly identical nonlinear elastic response, has enabled us to qualitatively explore the feasibility of our scheme without a to carryout a full 3D simulation. Our approach will enable us to study the feasibility of doing this reconstruction even if we do not know the exact microstructure of the material.

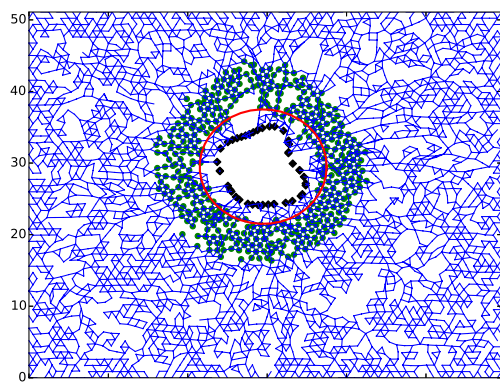
## II. MODELS AND SIMULATIONS



(a)



(b)



(c)

FIG. 1. Details of the ECM deformation model: Shown in (a) is a diluted triangular lattice with  $p=0.57$ . In (b) a round cell embedded in the lattice; the green circles are the marker beads (we choose the ones in a range between 10 and 15 from the center of the cell) and the black diamonds are the attached nodes. In (c) we show the relaxed network, and the red circle is the initial cell boundary.

We model the ECM as a diluted triangular lattice (Fig 1 a). In this lattice, each bond, with stretching stiffness  $k$  and bending stiffness  $\kappa$ , exists stochastically with a probability  $p$ . The Hamiltonian is:

$$H = \sum_{\langle i,j \rangle} \frac{k}{2a} g_{ij} (|\mathbf{R}_{ij}| - a)^2 + \sum_{\langle i,j,k \rangle} \frac{\kappa}{2a} g_{ij} g_{jk} \Delta\theta_{ijk}^2$$

in which  $a$  is the natural length of each bond.  $g_{ij} = 1$  when the bond between node  $i$  and  $j$  is present and  $g_{ij} = 0$  when the bond is removed. The first term refers to the stretching energy:  $\langle i,j \rangle$  sums over all neighboring lattice sites and  $|\mathbf{R}_{ij}|$  is the length of bond in deformed state. The second term represents the bending energy:  $\langle i,j,k \rangle$  sums over all groups of three co-linear consecutive lattice sites in the reference state and  $\Delta\theta_{ijk}$  is the change of angle in the deformed state. In such a lattice,  $p$  satisfies  $pZ = \langle z \rangle$ ,  $Z$  is the coordination number, which is 6 for a triangular lattice, and  $\langle z \rangle$  is the average connectivity of biopolymer networks. Since experiments have shown  $\langle z \rangle \approx 3.4$  [31], we set  $p = 0.57$  in our model.

We insert a round cell into the network by cutting a circular hole in the middle (Fig 1 b). The intersections between the cell boundary and network bonds are the attached nodes, which connect the cell with its ECM environment. Each one of these nodes can be located by its angular position in the circular cell boundary. Then we stretch the cell in the normal directions (Fig 1 c); for the  $i$  th attached node, its displacement towards cell center satisfies:

$$d(\theta_i, \mathbf{P}) = A_0 + \sum_{n=1}^N (A_n \cos(n\theta_i) + B_n \sin(n\theta_i))$$

in which  $\theta_i$  is the position of the  $i$  th node,  $\mathbf{P} = (A_0, A_1, \dots, A_N, B_0, \dots, B_N)$  are the determining parameters of cell stretching and the length of  $\mathbf{P}$  is the number of degrees of freedom. The above formula accounts for the fact that spatially close attached nodes should undergo similar displacements to preserve the smoothness of cell membrane. Hence, we limit ourselves to relatively few large wavelength modes in setting the cell boundary deformation.

Once the cell is deformed, we relax the lattice into its energy minimum state by the conjugate gradient method. Each parameter setting  $\mathbf{P}$  leads us to a particular cell stretching pattern:

$$\mathbf{d}(\mathbf{P}) = (d(\theta_1, \mathbf{P}), d(\theta_2, \mathbf{P}), \dots, d(\theta_N, \mathbf{P}))$$

which results in ECM deformation. In our scheme, we assume that ECM deformation is measured through the displacements a set of  $M$  marker beads, as following:

$$\mathbf{D}(\mathbf{P}) = (\mathbf{u}_1, \mathbf{u}_2, \dots, \mathbf{u}_M)$$

We stochastically set the parameters  $\mathbf{P} = \mathbf{P}_{set}$  and generate the corresponding "observed" displacements of

marker beads  $\mathbf{D}_{observed}$ . By minimizing

$$f = \|\mathbf{D}(\mathbf{P}_{guess}) - \mathbf{D}_{observed}\|^2$$

we can approximate the  $\mathbf{P}_{set}$  with  $\mathbf{P}_{guess}$ , thus realizing the reconstruction. To minimize the function  $f$ , we apply a combination of Particle Swarm Optimization (PSO) [32] and downhill simplex algorithm: we first run the PSO search for several times and pick the best value reached, and then we run the downhill simplex algorithm to further minimize the error function  $f$ .

### III. RESULTS

We carry out most of our simulations in a  $60 \times 60$  lattice, with  $p = 0.57$ ; to eliminate the possible boundary effects from the lattice, we verified that a  $100 \times 100$  lattice gives similar results. We set the lattice segment length to be  $a$  and our round cell has an initial radius  $R_0 = 8a$ . Physically,  $a$  is corresponding to the persistent length of collagen fibers ( $\approx 1\mu\text{m}$ ). As already mentioned, we maintain the smoothness of cell membrane by limiting deformation to the  $N$  longest wavelength modes when stretching the cell:

$$\mathbf{P} = (A_0, A_1, A_2, \dots, A_N, B_1, B_2, \dots, B_N)$$

We fix  $A_0 = a_0 + a\xi$  and  $A_i, B_i = 0.5a\xi$  ( $i = 1, 2, \dots, N$ ), and  $\xi$  is a stochastic variable uniformly distributed between 0 and 1. A constant  $a_0$  (usually around  $2a$  to  $3a$  in our simulations) is added to make sure that the cell contracts mostly, as most cells studied in such ECM systems are contractive. To track the ECM deformation, we initially let all lattice sites be inhabited by marker beads. We solve the inverse problem of "what stretching pattern leads to the observed beads' displacements with Particle Swarm Optimization and the downhill simplex algorithm.

Since the Particle Swarm Optimization algorithm applies a stochastic searching strategy, instead of giving a "Yes or No" answer, we will measure how likely the reconstruction will be successful by running the same simulation for dozens of times with different random seeds. Here, by "a successful reconstruction", we refer to the predictions for all attached nodes on the cell membrane deviating by no more than 5% from the input data. In addition, the chances to succeed for a PSO procedure will always increase as the number of searching rounds and ideally one can always get to the right answer with an infinite amount of computer time. Due to limited resources, also for the sake of comparison, we assign at most 3 rounds of PSO search with a maximum of 100 steps in each simulation, followed by the downhill simplex method.

We run groups of 20 simulations for a variety of  $N$  values. The results indicate the existence of a limit of resolution in our scheme for spatial frequencies. Our scheme works well if the morphology change of cell is restricted to the 4 or 5 longest wavelength modes. The algorithm

experiences a sharp drop in performance when stretching at higher frequencies is present (Fig 2). This is to say, if a cell changes its shape in a highly noncontinuous way, the reconstruction of cellular forces will become extremely hard. Given the continuous nature of cell membrane, this is unlikely to occur.

Errors are unavoidable in all kinds of experimental measurements. We therefore test the robustness of our scheme in the face of errors in the determination of the ECM deformation. We stochastically disturb the positions of all marker beads by some percentage of bond length after the network has relaxed to its energy-minimized state, and then do the inverse problem with the disturbed beads' displacement data. We found significant robustness to our reconstruction, with accurate forces able to be found even with noise as big as 30% (see Fig 3a). A second possible source of error is a mistaken value of the parameters of the system. We therefore carry out the forward and inverse problems with different values of the stretching and bending stiffnesses. As can be seen in Fig 3b, our scheme gives robust answers with stretching and bending stiffness changes of roughly 10%. These results are encouraging as we plan in future work to carry out the inversion for actual (rather than simulated) experimental data.

To study the relation between the reconstruction efficiency and the distribution of beads, we start by "turning off" the marker beads far away from the cell center ( $> R_{max}$ ). Noise-free simulations of  $R_{max} = 10, 15, 20, 25$  all lead to perfect performances, indicating that sampling the whole network with marker beads is not necessary for a successful reconstruction. To further investigate the effects of the distribution of marker beads near the cell, we keep only the marker beads within a range of  $R_{min}$  to  $R_{max}$  from the center of the cell. As seen in Table 1, elimination of beads that are within a range of 10 to 15 will lead to a sharp drop in reconstruction performance, which means marker beads near the cell are not equally important in our scheme: the closer, the more important. In addition, inversion attempts with both randomly and regularly diluted (up to 50%) distributions of beads in the neighborhood of the cell suffer no decrease in performance, showing the insensitivity of our scheme towards bead density.

TABLE I. Relation between bead positions and reconstruction performance (with 5% noise)

$R_{min}$	$R_{max}$	performance
0	10	100%
0	15	100%
10	15	100%
15	20	40%
20	25	40%

As we have discussed above, the response of the ECM to cell-induced deformation is non-linear and non-affine. This is ultimately due to the fact that the network is

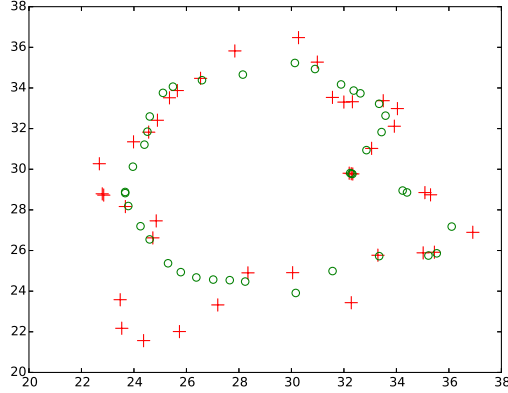
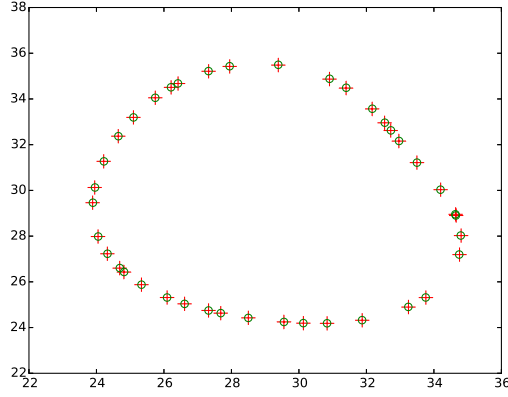
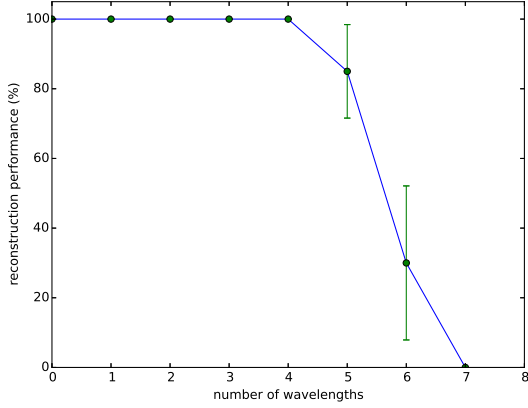


FIG. 2. Smoothness resolution. (a) Relation between number of longest modes considered in cell stretching and reconstruction performance ( $N=0$  refers to uniform stretching of the cell) and the probability of successful reconstruction. (b) A typical reconstruction result with 3 ( $N=3$ ) longest modes considered: green circles are their relaxed positions of attached nodes and the red crossings are the predicted positions of them. (c) An inaccurate reconstruction result with 7 modes considered ( $N=7$ )

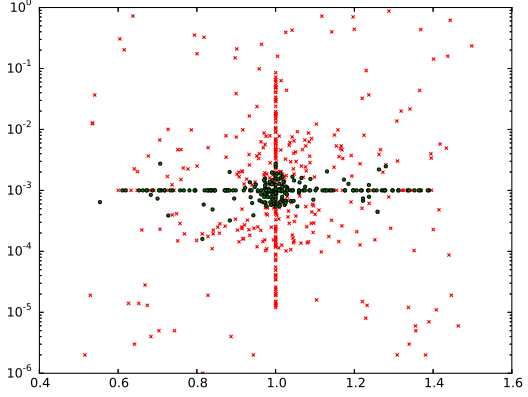
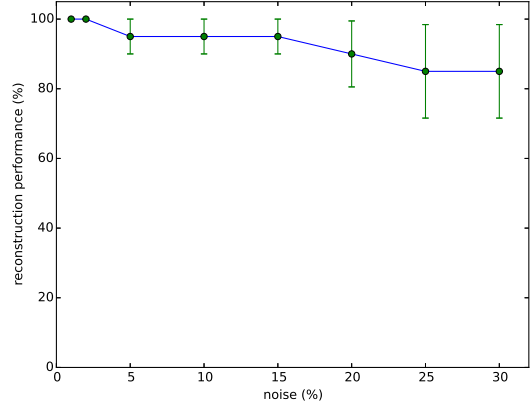


FIG. 3. Performance against errors. (a) simulated probability of successful reconstructions ( maximum deviation less than 5 %) with different fluctuation strengths of marker beads' positions. (b) Robustness in case of error of stretching and bending stiffness ( $k, \kappa$ ); the green dots are values of the stiffnesses used in the inverse algorithm leading to correct reconstructions, while red 'x' signs are the values leading to failed reconstructions.

below the Maxwell point and hence exhibits a transition from bending-dominated to stretching-dominated as strain is increases and the fibers become more aligned. A second feature is that the ECM, both in our model and in experiment, is highly heterogeneous on the cellular scale. The first point argues against being able to accurately invert the bead displacements by using linear elastic models. To figure out how much this matters in practice, we compare our results with calculations on a full triangular lattice, with all bonds present except for the ones attached to the cell membrane, representing an approximately affine reference model, and perform our comparison in two ways: one forward and one backward. In the forward comparison, we contract our cell exactly the same way in a diluted lattice and a full lattice and compare the displacements of marker beads, in a range between 10 and 15 from the center of the cell. As seen in Fig 4(a-c), large deviations in network responses are

observed in these areas close to the cell. In the backward perspective, we relax our system on a diluted lattice and then attempt to recover the cell deformation based on a full lattice (Fig 5(a,b) ); this would be analogous to doing the inverse problem with a linear elastic model. In all of our 20 attempts, reconstruction fails with very large deviations, up to 175% (Fig 5 (c) ). Our conclusion is that naive reconstructions will be highly inaccurate.

we next turn to the second issue, that of heterogeneity. It is obvious that the details of the actual microstructure will vary from realization to realization, even for networks that are statistically the same. Hence it is important to ask whether one needs to know a detailed model of the specific ECM or whether having a model in the same class is sufficient. This question is connected as well to whether a nonlinear continuum model which gets the correct macroscopic properties of the network can suffice for the inversion problem. To answer this question, we apply a similar strategy to our study of non-affine effects. We compare the responses to a same deforming cell of two ECM networks with the same dilution but different network connectivity. As seen in Fig 5(a), deformations may differ with a magnitude about twice the bond length in these two cases. In addition, we relax the cellularized network with one lattice, while reconstructing cell contraction based on a differently connected network, keeping the bulk properties invariant. Similarly to the above affinity case, all simulations, without exception, lead to considerably wrong predictions. (Fig 5(b) ). Therefore, merely knowing the bulk properties will not lead one to correct force reconstruction, unless micromechanical information of the ECM is estimated to some extent.

So far, all our studies have focused on the normal contraction of round cells. In reality however, cells often display long protrusive structures, pulling on the ECM networks. As a simple extension of our model, we have also studied elliptical cells. We allow an elliptical cell to move, while shrinking in its long axis. For this case, our simulations can quickly converge to the correct reconstruction. (Fig 6(a,b) ). Noticing that slight tangential movements are also possible, we also verify that our scheme works for a uniformly rotated round cell ( Fig 6(c,d) ).

## DISCUSSION

For motion on two-dimensional surfaces, the method of traction force microscopy has given unprecedented insight into the way cells use their active cytoskeletal machinery to interact with the surface (and, in the case of collective motion, with each other). It is therefore only natural to try to extend this methodology to cells moving within three-dimensional matrix materials. There are of course microscopy challenges in measuring the deformation of the matrix, but here for the sake of argument we have assumed that we can gather this information. Instead we ask a different question, namely how does the

known mechanical complexity of the ECM material limit our ability to invert deformations to find forces?

We have therefore explored the feasibility of reconstructing cell-generated forces from ECM deformation based on a mechanical ECM model. Our model, based on a diluted triangular lattice which has been shown to be able mimic both macroscopic properties of the lattice rheology such as strain-stiffening and alignment but also local heterogeneities on the scale of individual cells. The results have shown both good and bad news for moving forward with this proposed inversion. On the one hand, we show the effectiveness and robustness of our inversion scheme. As long as we do not demand too high a spatial resolution, we can show that marker deformations do indeed cellular contractions. This limitation is not too surprising. We can imagine a pair of close neighboring adhesion sites on the cell membrane which undergo very different stretching; if they exchange their stretching, almost the same displacements of marker beads will be observed, thus making it too hard to distinguish the different configurations in the reconstruction. That explains why a relatively smoother stretching configuration, where close neighbors bonds stretch almost the same, will suffer much less from this degeneracy. Fortunately, the fact cell membrane is relatively smooth should keep us from worrying too much about these troublesome degeneracies. Finally, though we limit our investigation in 2D, we believe a 3D version will exhibit similar physics.

Any experiment based reconstruction must be robust with respect to expected uncertainties in measurement and in assumed material properties. Our scheme does well in filtering out the fluctuations of bead displacements. As for any error in the assumed values of the stretching and bending stiffnesses, the performance shows a relatively higher sensitivity to stretching over bending. This is presumably because the strain induced by the cell is high enough to put the nearby lattice in a stretching dominated regime and is it these nearby points which are most important for the inversion. This is also consistent with our study of the effects of limitations on the available marker measurements.

Now for the bad news. To bridge the gap between our scheme and experiments, several more questions need to be addressed more carefully. We have shown that one needs to do a decent job on the actual microstructure of the lattice, not just on its average properties. We showed this by using a different realization of the network geometry to do the inversion and noted that there were rather severe inaccuracies. This of course depend on the details of the ECM geometry and specifically on the size of the cell versus the scale of the lattice microstructure. Our results, chosen for parameters which does a good job of reproducing the micro-mechanical variation for typical collagen 1 gels, show however that this can be a real limitation. One approach would be to measure the detailed micromechanics and use this information to guide lattice construction. To our knowledge, microstructures of collagen networks can be imaged through confocal reflec-

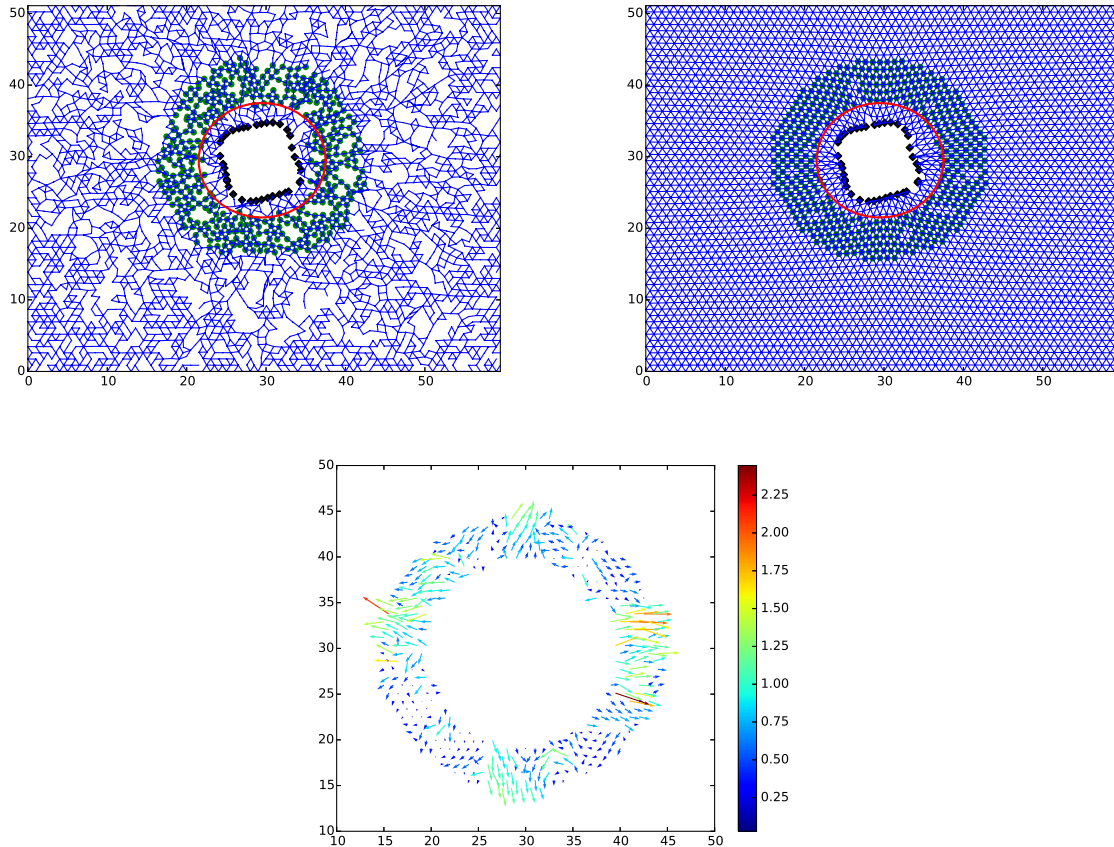


FIG. 4. Non-affine effects on reconstruction, forward comparison: different deformations are induced by the same contracting cell in a  $p=0.57$  ECM (a) and a  $p=1.0$  ECM (b) (All attached nodes remain invariant) red circles are the initial cell boundary, black diamonds are the attached nodes, the green circles refer to the visible points (c) shows the difference between marker deformations in the two cases.

tion microscopy [33–35] , and optical trap methods could help extract micromechanical information in the ECM [10]. Clearly, we do not know at present how these data can be "written" into a model for force reconstruction.

## CONCLUSION

In summary, we have developed a computational scheme to reconstruct cellular forces in a cell-ECM sys-

tem. The guiding principle of our scheme is to model the ECM response to cell-generated forces with a simple lattice-based model. Our scheme demonstrates robustness against noise in marker beads measurements and systematic errors of material characterization. Results of our 2D exploration elucidate how non-affine effects affect the reconstruction accuracy. Also we argue that the micromechanical properties of ECM may be crucial for a precise reconstruction.

## ACKNOWLEDGMENTS

---

[1] P. Friedl, K. S. Zänker, and E.-B. Bröcker, *Microscopy Research and Technique* **43**, 369 (1998), ISSN 1059-910X.

[2] B. Alberts, A. Johnson, J. Lewis, M. Raff, K. Roberts, and P. Walter (2002).

[3] M. Dembo and Y.-L. Wang, *Biophysical journal* **76**, 2307 (1999).

[4] R. W. Style, R. Boltyanskiy, G. K. German, C. Hyland, C. W. MacMinn, A. F. Mertz, L. A. Wilen, Y. Xu, and E. R. Dufresne, *Soft Matter* **10**, 4047 (2014), ISSN 1744-683X, URL <http://xlink.rsc.org/?DOI=c4sm00264d>.

[5] W. R. Legant, J. S. Miller, B. L. Blakely, D. M. Cohen, G. M. Genin, and C. S. Chen, *Nature methods* **7**, 969 (2010), ISSN 1548-7105.

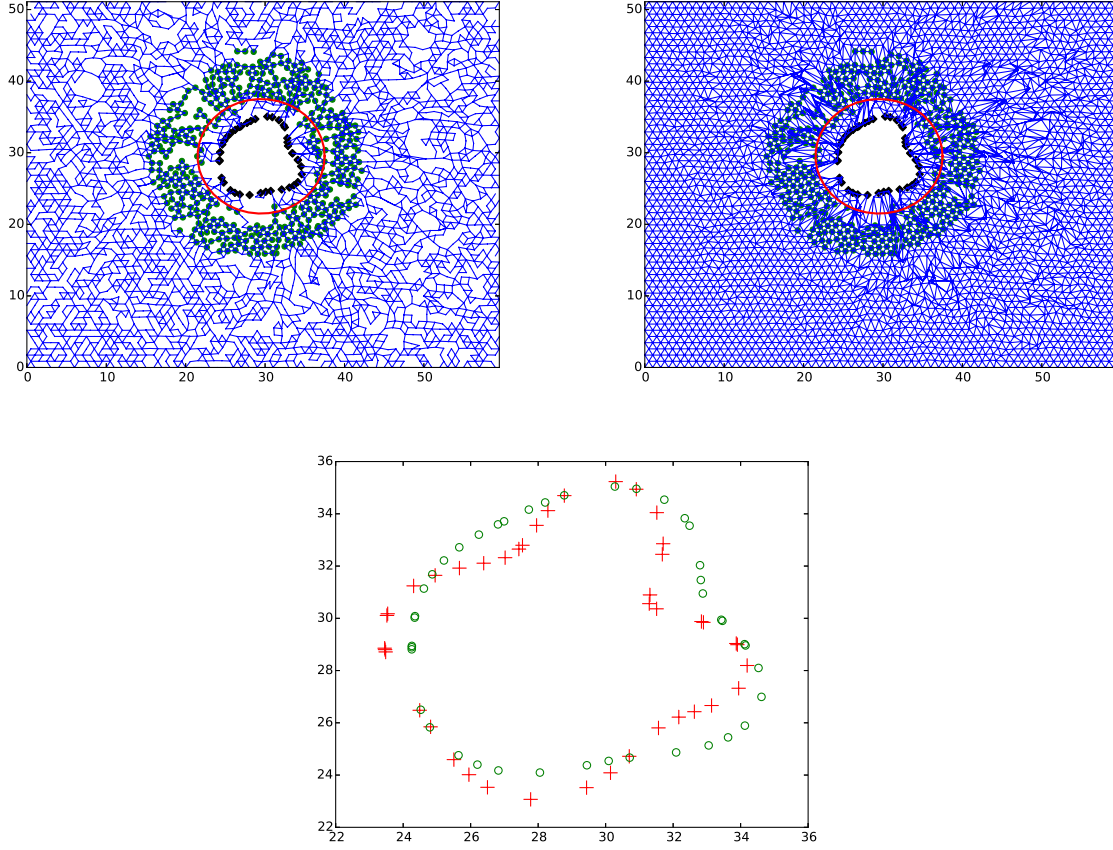


FIG. 5. Nonaffine effects on reconstruction: Backward comparison: if a relaxed ECM system (d) is reconstructed based on a full connectivity model (e), a highly inaccurate reconstruction will be achieved (f); red circles are the initial cell boundary, black diamonds are the attached nodes, the green circles refer to the visible points. In (e) the green hollow circles are the relaxed positions of all attached nodes, and the red crossings represent the predicted positions of them

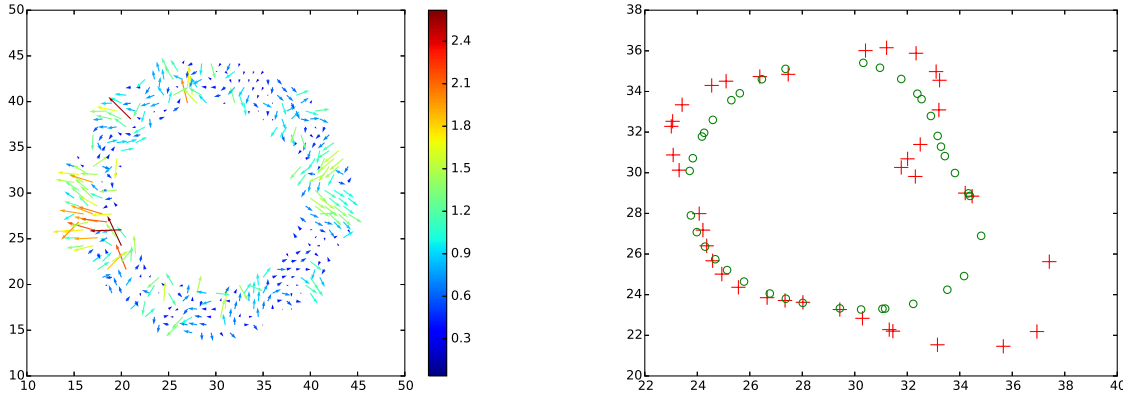


FIG. 6. Network connectivity's effects on reconstruction: Similar to Figure 4(c), two different network connectivities both with  $p=0.57$  will lead to large differences in the ECM deformation(a). Also, reconstruction of cellular forces based on a different network connectivity as compared with the original one leads to very inaccurate reconstructions (b): the green hollow circles are the relaxed positions of all attached nodes, and the red crossings represent the predicted positions of them

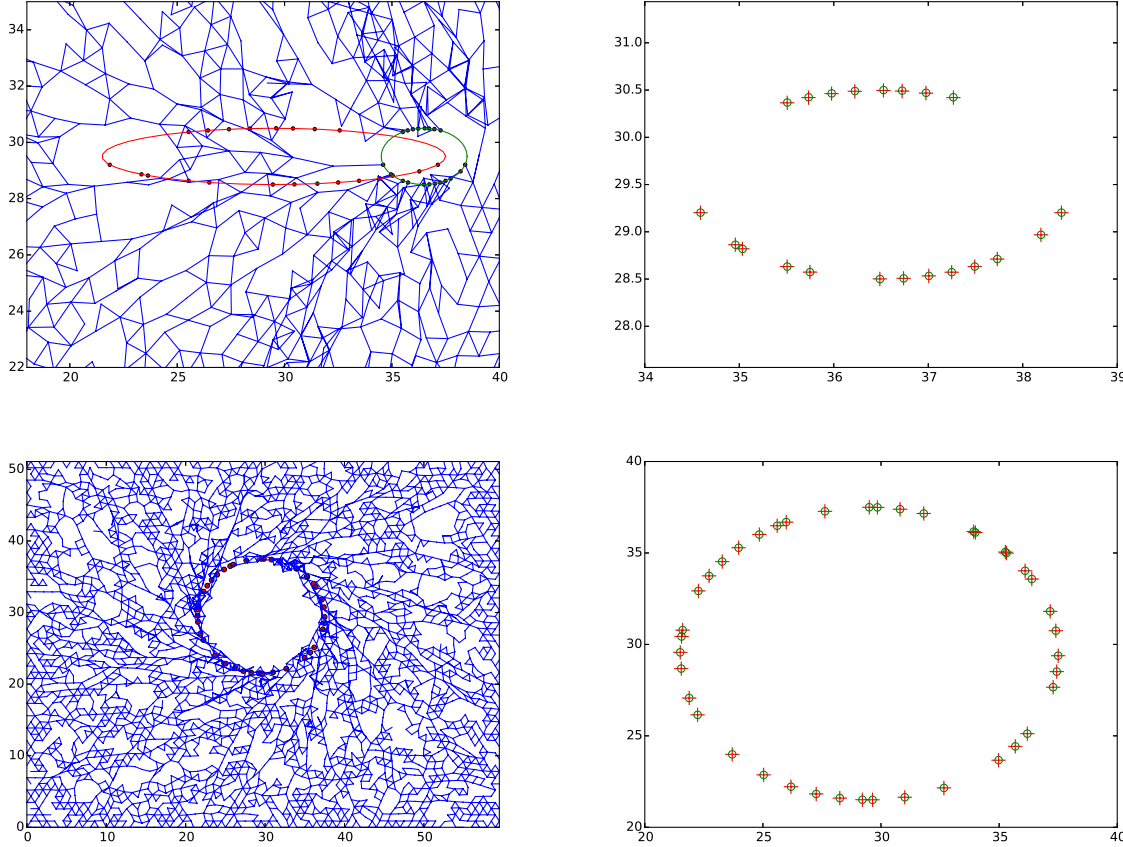


FIG. 7. Extensions of our scheme: (a-b)The migration and shrinking of an elliptic cell is accurately reconstructed ( we choose to plot only a portion of the ECM system with shrinking elliptic cell for clarity) (c-d)The uniform rotation of a circular cell (50 degrees) is accurately reconstructed: the green hollow circles are the relaxed positions of all attached nodes, and the the red crossings represent the predicted positions of them

- [6] J. Steinwachs, C. Metzner, K. Skodzek, N. Lang, I. Thievessen, C. Mark, S. Münster, K. E. Aifantis, and B. Fabry, *Nature Methods* **13**, 171 (2015), ISSN 1548-7091, URL <http://www.nature.com/doifinder/10.1038/nmeth.3685>.
- [7] R. A. Brown, *Experimental cell research* **319**, 2460 (2013), ISSN 1090-2422, URL <http://www.ncbi.nlm.nih.gov/pubmed/23856376>.
- [8] C. Storm, J. J. Pastore, F. C. MacKintosh, T. C. Lubensky, and P. A. Janmey, *Nature* **435**, 191 (2005), ISSN 0028-0836, URL <http://www.nature.com/doifinder/10.1038/nature03521>.
- [9] X. Feng and C.-Y. Hui, *Computational Mechanics* **58**, 91 (2016), ISSN 0178-7675, URL <http://link.springer.com/10.1007/s00466-016-1283-1>.
- [10] C. A. R. Jones, M. Cibula, J. Feng, E. A. Krnacik, D. H. McIntyre, H. Levine, and B. Sun, *Proceedings of the National Academy of Sciences* **112**, E5117 (2015), ISSN 0027-8424, URL <http://www.pnas.org/lookup/doi/10.1073/pnas.1509663112>.
- [11] C. Broedersz and F. MacKintosh, *Reviews of Modern Physics* **86**, 995 (2014), ISSN 0034-6861, URL <http://link.aps.org/doi/10.1103/RevModPhys.86.995>.
- [12] C. P. Broedersz, X. Mao, T. C. Lubensky, and F. C. MacKintosh, *Nature Physics* **7**, 983 (2011), ISSN 1745-2473, URL <http://www.nature.com/doifinder/10.1038/nphys2127>.
- [13] C. P. Broedersz and F. C. MacKintosh, *Soft Matter* **7**, 3186 (2011), ISSN 1744-683X, URL <http://xlink.rsc.org/?DOI=c0sm01004a>.
- [14] C. P. Broedersz, M. Sheinman, and F. C. MacKintosh, *Physical Review Letters* **108**, 078102 (2012), ISSN 0031-9007, URL <http://link.aps.org/doi/10.1103/PhysRevLett.108.078102>.
- [15] C. Heussinger and E. Frey, *Physical Review E* **75**, 011917 (2007), ISSN 1539-3755, URL <http://link.aps.org/doi/10.1103/PhysRevE.75.011917>.
- [16] X. Mao, O. Stenull, and T. C. Lubensky, *Physical Review E* **87**, 042602 (2013), ISSN 1539-3755, URL <http://link.aps.org/doi/10.1103/PhysRevE.87.042602>.
- [17] J. Feng, H. Levine, X. Mao, and L. M. Sander, *Physical Review E* **91**, 042710 (2015).
- [18] J. Feng, H. Levine, X. Mao, and L. M. Sander, *Soft Matter* pp. 1419–1424 (2016).
- [19] M. Vahabi, A. Sharma, A. J. Licup, A. S. van Oosten, P. A. Galie, P. A. Janmey, and F. C. MacKintosh, arXiv

preprint arXiv:1603.03239 (2016).

[20] A. Sharma, A. Licup, K. Jansen, R. Rens, M. Sheinman, G. Koenderink, and F. MacKintosh, *Nature Physics* (2016).

[21] E. Conti and F. C. MacKintosh, *Physical Review Letters* **102**, 088102 (2009), ISSN 0031-9007, URL <http://link.aps.org/doi/10.1103/PhysRevLett.102.088102>.

[22] J. Wilhelm and E. Frey, *Physical Review Letters* **91**, 108103 (2003), ISSN 0031-9007, URL <http://link.aps.org/doi/10.1103/PhysRevLett.91.108103>.

[23] D. A. Head, A. J. Levine, and F. C. MacKintosh, *Physical Review E* **68**, 061907 (2003), ISSN 1063-651X, URL <http://link.aps.org/doi/10.1103/PhysRevE.68.061907>.

[24] D. A. Head, A. J. Levine, and F. C. MacKintosh, *Physical Review Letters* **91**, 108102 (2003), ISSN 0031-9007, URL <http://link.aps.org/doi/10.1103/PhysRevLett.91.108102>.

[25] P. R. Onck, T. Koeman, T. van Dillen, and E. van der Giessen, *Physical Review Letters* **95**, 178102 (2005), ISSN 0031-9007, URL <http://link.aps.org/doi/10.1103/PhysRevLett.95.178102>.

[26] E. M. Huisman, C. Storm, and G. T. Barkema, *Physical Review E* **78**, 051801 (2008), ISSN 1539-3755, URL <http://link.aps.org/doi/10.1103/PhysRevE.78.051801>.

[27] A. Shahsavari and R. C. Piciu, *Physical Review E* **86**, 011923 (2012), ISSN 1539-3755, URL <http://link.aps.org/doi/10.1103/PhysRevE.86.011923>.

[28] A. Abhilash, B. M. Baker, B. Trappmann, C. S. Chen, and V. B. Shenoy, *Biophysical journal* **107**, 1829 (2014).

[29] A. J. Licup, S. Münster, A. Sharma, M. Sheinman, L. M. Jawerth, B. Fabry, D. A. Weitz, and F. C. MacKintosh, *Proceedings of the National Academy of Sciences* **112**, 9573 (2015).

[30] A. J. Licup, A. Sharma, and F. C. MacKintosh, *Physical Review E* **93**, 012407 (2016), ISSN 2470-0045, URL <http://link.aps.org/doi/10.1103/PhysRevE.93.012407>.

[31] S. B. Lindström, D. A. Vader, A. Kulachenko, and D. A. Weitz, *Physical Review E* **82**, 051905 (2010).

[32] J. Kennedy, in *Encyclopedia of machine learning* (Springer, 2011), pp. 760–766.

[33] C. A. R. Jones, L. Liang, D. Lin, Y. Jiao, and B. Sun, *Soft Matter* **10**, 8855 (2014), ISSN 1744-683X, URL <http://xlink.rsc.org/?DOI=C4SM01772B>.

[34] A. O. Brightman, B. P. Rajwa, J. E. Sturgis, M. E. McCallister, J. P. Robinson, and S. L. Voigt-Harbin, *Biopolymers* **54**, 222 (2000), ISSN 0006-3525, URL <http://www.ncbi.nlm.nih.gov/pubmed/10861383>.

[35] J. Kim, C. A. R. Jones, N. S. Groves, and B. Sun, *PloS one* **11**, e0156797 (2016), ISSN 1932-6203.